EPR Spectra from "EPR-Silent" Species: High-Field EPR Spectroscopy of Aqueous Chromium(II)

Joshua Telser,*,† Luca A. Pardi,‡,§ J. Krzystek,‡ and Louis-Claude Brunel‡

Chemistry Program, Roosevelt University, Chicago, Illinois 60605, Center for Interdisciplinary Magnetic Resonance, National High Magnetic Field Laboratory, Florida State University, Tallahassee, Florida 32310, and Consorzio Interuniversitario Nazionale per la Scienza e Tecnologia dei Materiali, 50134 Florence, Italy

Received June 15, 1998

High-field (up to 14.5 T) multifrequency (∼90−440 GHz) electron paramagnetic resonance (EPR) spectroscopy has been used to probe the non-Kramers, $S = 2$, Cr^{2+} ion in frozen aqueous solution, in the presence and absence of the glassing agent, glycerol. Solutions with both chloride and sulfate counterions were investigated. Detailed analysis based on a combination of analytical and full-matrix solutions to the spin Hamiltonian for an $S = 2$ system gave zero-field splitting parameters $D = -2.20(5)$ cm^{-1}, $E = 0.0(1)$ cm^{-1}, and $g_\perp \approx g_\parallel = 1.98(2)$, independent of solvent system and counterion. These results are in agreement with an early single-crystal EPR study of $CrSO_4 \cdot 5H_2O$; however, the present study allows unequivocal determination of the sign of D and shows that in solution $[Cr(H_2O)_6]^{2+}$ is a perfectly axial system (tetragonally elongated), as opposed to solid $CrSO_4 \cdot 5H_2O$, which showed a measurable E value, indicative of slight orthorhombic distortion as seen in its crystal structure. HF-EPR data is combined with earlier electronic absorption data to provide a complete picture of the electronic structure of Cr^{2+} in this chemical environment. The results are also compared to a recent HF-EPR study of a Mn^{3+} complex, which showed that electronic excited states affect the ground state of the complex, but these effects are less pronounced for Cr^{2+}. The present study also shows the applicability of high-field EPR to aqueous solutions of integer-spin ("EPR-silent") transition metal complexes, as previous studies have employed only solid (single-crystal or polycrystalline) samples.

Introduction

EPR[1] spectroscopic methods at conventional microwave frequencies (X-band, ∼9 GHz (0.3 cm^{-1}); Q-band, ∼35 GHz (1.2 cm^{-1})) and magnetic fields (up to ∼1.5 T) have been fruitfully employed in determining the structural and electronic environments of half-integer-spin (Kramers) paramagnets. These methods, however, are not applicable to systems with integer-spin (non-Kramers) ground states, where the zero-field splitting (zfs) is larger than the microwave quantum, in particular where the zfs interaction approaches axial symmetry.[2] The recently developed technique of high-frequency, high-field EPR ($\nu >$ 90 GHz; B_0 up to ∼15 T)[3−11] has now proven to be effective at elucidating the electronic structure of integer-spin systems.[12−16] Of particular value is the combination of the multifrequency capability of the EPR spectrometer employed here (25−3000 GHz (∼100 cm^{-1})) with the ability to perform continuous field sweeps over a broad range (0−17 T). This allows one to chose a convenient parameter "window" to observe most, if not all, of the multitude of transitions characterizing a high-spin, non-Kramers spin species.[17]

This study describes the use of HF-EPR to investigate a classic "EPR-silent" non-Kramers system, aqueous Cr^{2+} (HS $3d^4$, $S = 2$). We selected this system for its inherent interest as a high-spin system with Jahn−Teller distortion[2] and because a significant amount of background information on it exists.

† Roosevelt University.
‡ Florida State University.
§ Consorzio Interuniversitario Nazionale per la Scienza e Tecnologia dei Materiali.

(1) Abbreviations used are as follows: dbm, 1,3-diphenyl-1,3-propanedionate; ENDOR, electron nuclear double resonance; HF-EPR, high-field (frequency) electron paramagnetic resonance; HS, high-spin; LS, low-spin; zfs, zero-field splitting.

(2) Abragam, A.; Bleaney, B. *Electron Paramagnetic Resonance of Transition Ions*; Dover Publications: New York, 1986; pp 399, 434−436, 679.
(3) Gerfen, G. J.; Bellew, B. F.; Griffin, R. G.; Singel, D. J.; Ekberg, C. A.; Whittaker, J. W. *J. Phys. Chem.* **1996**, *100*, 16739−16748.
(4) Möbius, K. *Appl. Magn. Reson.* **1995**, *9*, 389−407.
(5) Smirnova, T. I.; Smirnov, A. I.; Clarkson, R. B.; Belford, R. L. *J. Phys. Chem.* **1995**, *99*, 9008−9016.
(6) Coremans, J. W. A.; Poluektov, O. G.; Groenen, E. J. J.; Canters, G. W.; Nar, H.; Messerschmidt, A. *J. Am. Chem. Soc.* **1996**, *118*, 12141−12153.
(7) Lebedev, Y. S. *Appl. Magn. Reson.* **1994**, *7*, 339−362.
(8) Lynch, W. B.; Boorse, R. S.; Freed, J. H. *J. Am. Chem. Soc.* **1993**, *115*, 10909−10915.
(9) Brunel, L.-C. *Physica B* **1995**, 360−362.
(10) Brunel, L. C.; Barra, A. L.; Martinez, G. *Physica B* **1995**, *204*, 298−302.
(11) Krzystek, J.; Sienkiewicz, A.; Pardi, L.; Brunel, L.-C. *J. Magn. Reson.* **1997**, *125*, 207−211.
(12) Goldberg, D. P.; Telser, J.; Krzystek, J.; Montalban, A. G.; Brunel, L.-C.; Barrett, A. G. M.; Hoffman, B. M. *J. Am. Chem. Soc.* **1997**, *119*, 8722−8723.
(13) Barra, A. L.; Caneschi, A.; Gatteschi, D.; Sessoli, R. *J. Am. Chem. Soc.* **1995**, *117*, 8855−8856.
(14) Barra, A.-L.; Gatteschi, D.; Sessoli, R.; Abbati, G. L.; Cornia, A.; Fabretti, A. C.; Uytterhoeven, M. G. *Angew. Chem., Intl. Ed. Engl.* **1997**, *36*, 2329−2331.
(15) Rentschler, E.; Gatteschi, D.; Cornia, A.; Fabretti, A. C.; Barra, A. L.; Shchegolikhina, O. I.; Zhdanov, A. A. *Inorg. Chem.* **1996**, *35*, 4427−4431.
(16) Caneschi, A.; Gatteschi, D.; Sessoli, R.; Barra, A. L.; Brunel, L. C.; Guillot, M. *J. Am. Chem. Soc.* **1991**, *113*, 5873−5874.
(17) Krzystek, J.; Goldberg, D. P.; Pardi, L. A.; Telser, J.; Hoffman, B. M.; Brunel, L.-C. Manuscript in preparation.

10.1021/ic9806683 CCC: $15.00
Published on Web 10/07/1998

Over 30 years ago, Fackler and Holah[18−21] performed a very thorough series of studies on the electronic absorption spectra of a number of Cr(II) complexes, providing ligand field parameters for these systems based in part on structural and electronic data for isomorphous Cu(II) complexes, such as $CuSO_4 \cdot 5H_2O$. The crystal structure of $CrSO_4 \cdot 5H_2O$ has now been reported[22] and shows that Cr^{2+} has tetraaquo equatorial ligands and disulfato axial ligands and is thus effectively *trans*-$[Cr(H_2O)_4(SO_4)_2]^{2-}$, as occurs for $CuSO_4 \cdot 5H_2O$. More importantly, a remarkable EPR study was performed over 40 years ago on single-crystal $CrSO_4 \cdot 5H_2O$ using microwave frequencies of 27, 46, and 55 GHz.[23,24] The magnitude, although not the sign, of the zfs parameter D was determined, along with approximate g values. Quite recently, two HF-EPR studies have appeared on a very similar ion, Mn^{3+}, also in a HS $3d^4$, $S = 2$ environment. One was on polycrystalline samples of several porphyrinic compounds of Mn(III),[12] and the other was on polycrystalline [Mn(dbm)$_3$], where dbm is 1,3-diphenyl-1,3-propanedionate.[14] HF-EPR studies determined the magnitudes and signs of the zfs parameters of Mn^{3+}, as we describe here for aqueous Cr^{2+}.

The above EPR studies differ from the present one in a key aspect, besides the different complexes involved, namely in the use of single-crystal or polycrystalline samples as opposed to frozen solutions. Single-crystals are the ideal system for complete analysis but present considerable experimental difficulties in terms of both sample preparation and spectroscopic measurements. Polycrystalline samples are far more convenient and are acceptable for inorganic complexes but still are generally inappropriate for metallobiomolecules. Notwithstanding a remarkable recent study of single-crystal azurin using 95 GHz EPR/ENDOR,[6] metallobiomolecules are generally only EPR accessible in dilute aqueous solution. Furthermore, although polycrystalline samples should exhibit true powder pattern EPR spectra, due to the totally random orientation of the microcrystallites, this is not always the case in HF-EPR. The applied magnetic field can lead to torquing of the microcrystallites and a nonrandom set of orientations. This was observed in the study of Mn(III) porphyrinic complexes, in which case the reorientation was so extreme as to eliminate any orientations perpendicular to B_0.[12] In contrast, a frozen solution, such as studied here, presents a true powder pattern set of orientations.

Experimental Section

Synthesis. The procedure of Holah and Fackler[25] was used to prepare solutions of aqueous Cr^{2+} with sulfate and chloride counterions from Cr metal and concentrated sulfuric and hydrochloric acids, respectively. As pointed out by these workers, to prevent further oxidation to Cr^{3+}, high-purity chromium metal must be used (here electrolytic Cr chips, Alfa Puratronic, 99.997%). Fresh "robin's egg" blue solutions of Cr^{2+} were used for EPR spectroscopy (in some cases, degassed glycerol was added ∼30% v/v). It was not possible to examine quantitatively by UV−visible spectroscopy specific EPR solution samples, but estimated Cr^{2+} concentrations were ∼0.1−0.2 M. Bright-blue microcrystalline solids ($CrSO_4 \cdot 5H_2O$ and $CrCl_2 \cdot 4H_2O$) were also obtained and studied by EPR. Large, bright-blue crystals of $CrSO_4 \cdot 5H_2O$ were obtained by refrigeration under nitrogen for several months of an aqueous Cr^{2+} sulfate solution.

EPR Spectroscopy. HF-EPR spectra were recorded on a spectrometer analogous to that described by Mueller et al.[26] It has been briefly described[11] and will be elaborated on in a forthcoming paper.[27] The spectrometer has fundamental microwave frequencies of ∼95 and ∼110 GHz, from which higher harmonics can be also generated to yield approximate frequencies of 190, 220, 285, 330, 380, and 440 GHz. A set of high-pass filters removes the fundamentals and lower harmonics. Cr^{2+} solutions were placed in a Teflon sample holder and rapidly frozen, all under nitrogen atmosphere. The frozen sample was then quickly loaded into the spectrometer in air. All forms of Cr^{2+} (solution, powder, and single crystal) showed evidence by EPR, although not visibly, of a small amount of Cr^{3+} ($3d^3$, $S = 3/2$) impurity. EPR is extremely sensitive to such Kramers systems, but the Cr^{3+} signal is easily identified and does not interfere with the signals from Cr^{2+} (see Results). The Cr^{3+} signal in fact provides an internal standard for field calibration. As a result of the spread of resonances over the entire available magnet field range (14.5 T), relatively rapid field scans were required (∼0.3 T/min). This results in a field hysteresis as measured by monitoring the magnet power supply current. The hysteresis was accounted for by sweeping the field in both directions and assuming the resonance field as the average from the two scans. This procedure creates an error of <5 mT as checked by standards, which is over an order of magnitude less than the line width of the signals detected in aqueous Cr^{2+}.

EPR Analysis. The magnetic properties of an ion with $S = 2$ can be described by the standard spin Hamiltonian comprised of Zeeman and zfs terms.

$$H = \beta B \cdot \mathbf{g} \cdot S + D(S_z^2 - S(S+1)/3) + E(S_x^2 - S_y^2) \qquad (1)$$

We employed several methods to apply eq 1 in analyzing the experimental EPR spectra. Analytical solutions exist to calculate the energy levels for B_0 parallel or perpendicular to the principal zfs (z) axis of an $S = 2$ system.[28] Numerical methods were also used to calculate the EPR transition energies and probabilities from the eigenvalues and eigenvectors, respectively, obtained by diagonalization of the spin Hamiltonian matrix resulting from eq 1. A program written by Weihe[29] was used to generate powder pattern EPR spectra, allowing direct assignment of the observed EPR transitions. This program was also employed by Barra et al. in their analysis of [Mn(dbm)$_3$].[14]

Results

HF-EPR spectra were recorded at 10 K of aqueous Cr^{2+} at multiple microwave frequencies: at the fundamental frequencies of ∼95 and ∼110 GHz and at each of their second, third, and fourth harmonics. Representative spectra were also recorded at other temperatures, such as 5 and 20 K. Comparison among spectra within the resulting set allows a given EPR transition to be followed as a function of field and frequency. Such a complete set is shown in Supporting Information (Figure S1). Individual spectra recorded at ∼110 and at ∼330 GHz for [Cr-$(H_2O)_6$](SO_4) are shown in Figures 1a and 2a, respectively. At sufficiently high magnetic fields, all the EPR transitions will show linear behavior with the slope proportional to an effective g value for that transition and the energy intercept, Δ, corresponding to an effective zfs for the particular transition.[12] This is shown in Supporting Information, wherein the resonant field for each feature is plotted versus microwave frequency (Figure

(18) Fackler, J. P., Jr.; Holah, D. G. *Inorg. Chem.* **1965**, *4*, 954−958.
(19) Holah, D. G.; Fackler, J. P., Jr. *Inorg. Chem.* **1965**, *4*, 1112−1116.
(20) Holah, D. G.; Fackler, J. P., Jr. *Inorg. Chem.* **1965**, *4*, 1721−1725.
(21) Holah, D. G.; Fackler, J. P., Jr. *Inorg. Chem.* **1966**, *5*, 479−482.
(22) Vaalsta, T. P.; Maslen, E. N. *Acta Crystallogr.* **1987**, *B43*, 448−454.
(23) Ono, K.; Koide, S.; Sekiyama, H.; Abe, H. *Phys. Rev.* **1954**, *96*, 38−39.
(24) Ono, K. *J. Phys. Soc. Jpn.* **1957**, *12*, 1231−1238.
(25) Holah, D. G.; Fackler, J. P., Jr. *Inorg. Synth.* **1967**, *10*, 26−35.
(26) Mueller, F.; Hopkins, M. A.; Coron, N.; Grynberg, M.; Brunel, L.-C.; Martinez, G. *Rev. Sci. Instrum.* **1989**, *60*, 3681−3684.
(27) Hassan, A.; Pardi, L. A.; Krzystek, J.; Sienkiewicz, A.; Rohrer, M.; Brunel, L.-C. Manuscript in preparation.
(28) Baranowski, J.; Cukierda, T.; Jezowska-Trzebiatowska, B.; Kozłowski, H. *J. Magn. Reson.* **1979**, *33*, 585−593. We note that there is an error on p 586; the variable p_1 is incorrectly set equal to b_1 and should be set equal to B_1. This change is necessary to obtain a correct energy level diagram as shown in Figure 3.
(29) Jacobsen, C. J. H.; Pedersen, E.; Villadsen, J.; Weihe, H. *Inorg. Chem.* **1993**, *32*, 1216−1221.

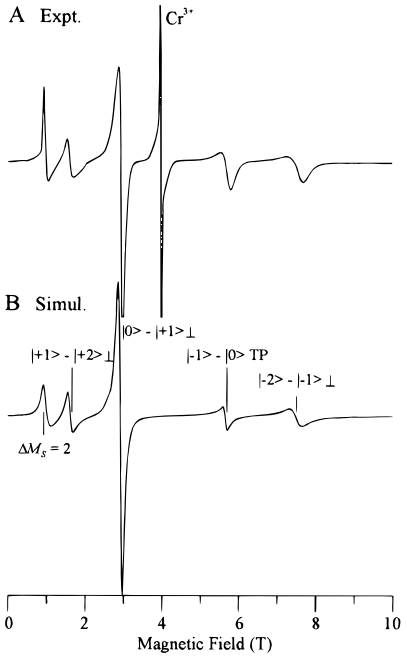

Figure 1. HF-EPR spectrum of aqueous Cr^{2+} (~0.1−0.2 M) with a sulfate counterion: (A) experimental spectrum; (B) simulated spectrum. (A) Experimental conditions: temperature, 10 K; microwave frequency, 109.564 GHz; field modulation frequency, 8.7 kHz; modulation amplitude, 1.5 mT; time constant, 0.3 s; scan rate, 0.3 T/min. The sharp signal from an aqueous Cr^{3+} impurity at $g = 2.00$ is indicated. (B) Simulation parameters: $S = 2$, $D = -2.2$ cm^{-1}, $E = 0$; $g_\perp = g_\parallel = 1.98$; single-crystal EPR line width, 100 mT. Fully allowed EPR transitions with $\Delta M_S = 1$ are assigned as to $|M_S\rangle$ ground and excited states and magnetic field orientation ($\parallel \equiv B_0$ along z, $\perp \equiv B_0$ along x) as indicated on the simulated spectrum. The resonance corresponding to $|-1\rangle \rightarrow |0\rangle$ occurs at an off-axis extremum or "turning point" when B_0 is ~60° from z and is so identified by the label TP. A partially allowed transition with $\Delta M_S = 2$ is also indicated.

S2). The slopes of several of these lines (traces B, D, F, G, and H in Figure S2) indicate that $g \approx 2$. This value is in agreement with the magnetic moments measured for several Cr^{2+} salts (e.g., for $CrSO_4 \cdot 5H_2O$, $\mu = 4.92(5)$;[18] $\mu = g(S(S+1)^{1/2} = 4.90$ for $S = 2$, $g = 2.00$), and the value $g \approx 2$ was obtained from the single-crystal EPR study of $CrSO_4 \cdot 5H_2O$.[23] Lines with significantly different slopes (traces C and E in Figure S2) correspond to partially allowed ($\Delta M_S > 1$) EPR transitions as assigned by computer simulation.

Temperature-dependent data show that transition B in Figure S2 arises from the ground state, which is either $|2, 0\rangle$ for $D > 0$ or $|2, -2\rangle$ for $D < 0$. The intercept of line B, $\Delta \approx 200$ GHz (~6.6 cm^{-1}), thus corresponds to either $\Delta = |D|$ for $D > 0$ or $\Delta = |3D|$ for $D < 0$.[12] As was previously found for both types of Mn(III) complex,[12,14] only $D < 0$ gives the observed behavior, in terms of matching both the overall EPR spectra and the temperature dependence of individual resonances, so that here $\Delta = |3D| \approx 6.6$ cm^{-1}. This value of $D = -2.2$ cm^{-1} is also in good agreement with the magnitude obtained previously for $CrSO_4 \cdot 5H_2O$ ($|D| = 2.24$ cm^{-1}).[23]

Use of a computer program written by Weihe[29] allowed assignment of all of the observed EPR transitions and refinement of the magnetic parameters for $[Cr(H_2O)_6]^{2+}$. The use of this program is particularly important in matching not only the frequencies but also the relative intensities of the EPR resonances. The corresponding simulated plots are shown in Figures 1b and 2b and employed the parameters $D = 2.20(5)$ cm^{-1}, $E = 0.0(1)$ cm^{-1}, and $g_\perp = g_\parallel = 1.98(2)$. The correspondence between the experimental and simulated spectra is excellent,

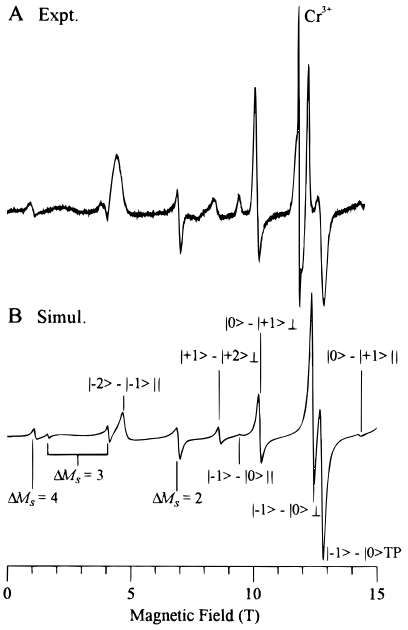

Figure 2. HF-EPR spectrum of aqueous Cr^{2+} with a sulfate counterion: (A) experimental spectrum; (B) simulated spectrum. (A) Experimental conditions: as in Figure 1a, except microwave frequency, 328.69 GHz. The sharp signal from an aqueous Cr^{3+} impurity at $g = 2.00$ is indicated. (B) Simulation parameters as in Figure 1b. EPR transitions are identified as in Figure 1b; at this higher microwave frequency, more transitions appear, including several with $\Delta M_S > 1$. Transitions corresponding to $|-1\rangle \rightarrow |0\rangle$ are observed with B_0 both along x ($\perp$) and at the turning point (TP), giving the observed "doubled" resonance.

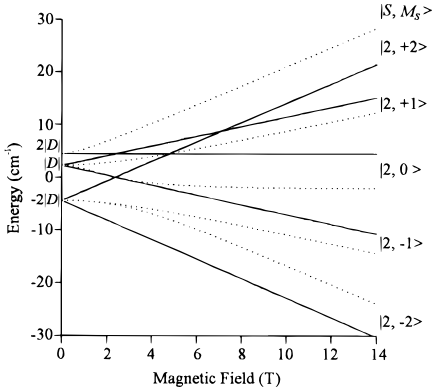

Figure 3. Energy level diagram for $[Cr(H_2O)_6]^{2+}$ using the spin Hamiltonian with $S = 2$, $D = -2.2$ cm^{-1}, $E = 0$, and $g_\perp = g_\parallel = 1.98$. The solid lines are the energies for B_0 along z ($B_\parallel$), and the dotted lines are those for B_0 along x ($B_\perp$). Specific $|S, M_S\rangle$ values are indicated, noting that these are pure state descriptions only for the states with $B_\parallel$. The energies are calculated using the equations of Baranowski et al.[28]

excepting of course the sharp signal due to the inevitable Cr^{3+} impurity. Although $g_\perp \neq g_\parallel$ is expected for an axial system, there was no improvement in the simulations by using, for example, $g_\perp = 1.96$ and $g_\parallel = 1.99$. Rather than arbitrarily impose a slightly axial **g** tensor, for simplicity, we use an isotropic $g = 1.98(2)$ for the spin Hamiltonian.

The energy levels of this $S = 2$ system using the simulation parameters are given in Figure 3, and the resulting EPR resonant energies are given in Figure 4. For convenience, the energy levels were calculated using the analytical solutions of Baranowski et al.,[28] while the EPR transition energies and probabilities were determined from the eigenvalues and eigenvectors obtained by diagonalization of the spin Hamiltonian matrix. These plots allow the assignment of the specific EPR transitions indicated in Figures 1 and 2 as well as those at any frequency.

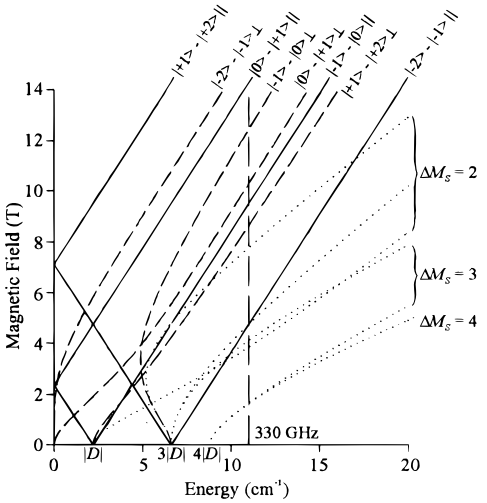

Figure 4. Plot of resonance field vs transition energy for $[Cr(H_2O)_6]^{2+}$ using the spin Hamiltonian with $S = 2$, $D = -2.2$ cm^{-1}, $E = 0$, and $g_\perp = g_{||} = 1.98$. The solid lines are the EPR resonance branches for B_0 along z ($B_{||}$), and the dashed lines are those for B_0 along x ($B_\perp$), both with $\Delta M_S = 1$ (fully allowed); the dotted lines are those for $B_\perp$ with $\Delta M_S > 1$ (partially allowed). The ground state $|M_S\rangle \rightarrow$ excited state $|M_S\rangle$ levels are indicated, based on the state assignments in Figure 3. The transition energies are calculated by diagonalization of the spin Hamiltonian matrix. The energy corresponding to 330 GHz is indicated by a dashed vertical line for comparison with the experimental spectrum in Figure 2a.

The information provided by these electronic parameters will be discussed below.

HF-EPR spectra of solutions of the chloride salt were essentially indistinguishable from those of the sulfate salt. This correspondence supports the identification made originally based on electronic absorption spectroscopy[18] that the aqueous solution species is indeed $[Cr(H_2O)_6]^{2+}$. Use of the glassing agent, glycerol, did not significantly alter the line shapes or line widths of the signals. Small differences between the experimental and simulated line shapes are inevitable due to a small, variable dispersion component in the former. Still, comparison of Figures 1a and 2a with Figures 1b and 2b shows that the overall line shape and line width match is quite good, although there are signals that appear slightly distorted in the experimental spectra (e.g., the transition labeled "$|1\rangle - |2\rangle\perp$" in Figure 2a). The success of the simulation at reproducing the experimental EPR line shape and line width, as well as the signal energies and intensities, clearly demonstrates that a HF-EPR spectrum of a frozen solution $S = 2$ system is as easily defined as a conventional EPR spectrum of a simple Kramers system. We do note, however, that at the very high magnetic fields employed here any "strain" (distribution in g values or other parameters) is greatly exacerbated, compared to conventional EPR. As a result, the line widths are unavoidably broad and the glass quality is relatively insignificant. Furthermore, the line breadth makes it quite difficult to determine g values with the precision typical for Kramers systems; however, as discussed below, zfs parameters provide the key information for understanding electronic structure in non-Kramers systems.

HF-EPR spectra were also obtained for polycrystalline $CrSO_4 \cdot 5H_2O$ and $CrCl_2 \cdot 4H_2O$. In this case, in contrast to the results observed for the frozen solution samples, the appearance of the spectra recorded for these samples is quite unusual, as seen in Figure S3. The difficulty is that, despite grinding the crystallites under nitrogen, a classical powder pattern is not obtained. The spectrum is dominated by the feature arising from the $|2, -2\rangle \rightarrow |2, -1\rangle$ transition with B_0 along z ($B_{||}$) that occurs near 4 T at 323 GHz (Figure S3a), which corresponds directly to that seen in the frozen solution (Figure 2a). At magnetic fields above this value, individual EPR signals are observed from microcrystallites with orientations such that the magnetic field "moves" in discrete steps from $B_{||}$ to $B_\perp$. The effect is identical to what would result from a computer-simulated powder pattern that does not sum a sufficient number of single-crystal orientations.[30] This experimental effect makes analysis of HF-EPR spectra from these solid samples problematic; however, the correspondence in resonant fields for both the $|2, -2\rangle \rightarrow |2,-1\rangle$ transition and the nominally forbidden $\Delta M_S = 4$ transition at ~1 T between the frozen solution and powder pattern samples indicates that the electronic parameters for solid $CrSO_4 \cdot 5H_2O$ and $CrCl_2 \cdot 4H_2O$ (which has four equatorial aquo and two axial chloro ligands[31]) are roughly the same as those for the hexaaquo solution species. We note that it is in principle possible to achieve a random distribution of microcrystallites by reducing their size, e.g., by grinding and immobilizing them in zero field by a convenient waxlike agent. This was recently done on solid Mn(III) complexes, which had previously aligned 100% with the field so that only parallel resonances were detected.[17] We finally note that high-quality HF-EPR spectra were also obtained for single-crystal $CrSO_4 \cdot 5H_2O$; however, a full angular dependence was not performed.

Discussion

Analysis of the multifrequency HF-EPR data set for aqueous Cr^{2+} combined with computer simulation provided the following parameters from eq 1: $D = -2.20$ cm^{-1}, $E = 0$, and $g_\perp = g_{||} = 1.98$. The pioneering single-crystal EPR study of $CrSO_4 \cdot 5H_2O$ similarly gave $|D| = 2.24$ cm^{-1}, $|E| = 0.1$ cm^{-1}, $g_\perp = 1.99$, and $g_{||} = 1.95$.[23,24] As described above, we have been able to determine unequivocally the sign of D, which was not possible in the earlier study. The fact that the parameters for the two complexes are not identical is likely the result of the chemical/structural difference between them.

X-ray crystallography shows that the Cr^{2+} ion in $CrSO_4 \cdot 5H_2O$ is axially coordinated by sulfato oxygen ($Cr-O_{sulfato}$ distances for each of the two Cr nonequivalent Cr sites are 2.4209(8) and 2.4578(8) Å, respectively) and equatorially coordinated by aquo oxygen ligands ($Cr-O_{aquo}$ distances are 2.0518(12) and 2.0532(8) Å for one Cr site and 2.0307(11) and 2.0529(8) Å for the other).[22] The significant difference between the axial and equatorial Cr−O bond lengths indicates a static Jahn−Teller distortion.[22] As pointed out by Fackler and Holah,[18] an octahedral complex can be tetragonally distorted by elongation of any pair of axial bonds, all of which are the same in $[Cr(H_2O)_6]^{2+}$ or CrX_2 (X = halide) but not in $CrSO_4 \cdot 5H_2O$. In $CrSO_4 \cdot 5H_2O$, the chemical difference between the axial and the equatorial ligands might also contribute to the different bond lengths (~0.4 Å); however, a similar tetragonal distortion (0.5 Å) is found in both $CrCl_2$[32] and CrI_2,[33] for which the six Cr−X bond lengths are divided into a set of four of 2.40 (X = Cl), 2.74 (X = I) Å and two of 2.91 (X = Cl), 3.24 (X = I) Å. (As a result of antiferromagnetic ordering, which has been previously studied by neutron diffraction,[34] HF-EPR of solid $CrCl_2$ was

(30) Mombourquette, M. J.; Weil, J. A. *J. Magn. Reson.* **1992**, *99*, 37−44.
(31) Runciman, W. A.; Syme, R. W. G. *Philos. Mag.* **1963**, *8*, 605−613.
(32) Tracy, J. W.; Gregory, N. W.; Lingafelter, E. C.; Dunitz, J. D.; Mez, H.-C.; Rundle, R. E.; Scheringer, C.; Yakel, H. L., Jr.; Wilkinson, M. K. *Acta Crystallogr.* **1961**, *14*, 927−929.
(33) Tracy, J. W.; Gregory, N. W.; Stewart, J. M.; Lingafelter, E. C. *Acta Crystallogr.* **1962**, *15*, 460−463.
(34) Cable, J. W.; Wilkinson, M. K.; Wollan, E. O. *Phys. Rev.* **1960**, *118*, 950−955.

Table 1. Electronic Parameters (in cm^{-1}) for Jahn−Teller Distorted $3d^4$ [9] Ions[a]

complex	D_q	D_s	D_t	D	E	g_z	$g_{x,y}$
$[Cr(H_2O)_6]^{2+}$ [b]							
exptl	1390	1740	470	−2.20(1)	0.0(1)	1.98(2)	1.98(2)
calcd method 1[c]				−2.04		1.97	1.99
calcd method 2[d]				−0.77		1.97	1.99
calcd method 3[e]				−2.62 (−2.66)			
$Cr\{Cu\}(SO_4)\cdot 5H_2O$[f]							
exptl	{1300}	{1710}	{730}	−2.24	0.1	1.95	1.99
calcd method 1[c]				−2.08		1.97	1.99
calcd method 2[d]				−0.80		1.97	1.99
calcd method 3[e]				−2.89 (−2.94)			
$[Mn(H_2O)_6]^{3+}$ [g]	1860	2530	600				
$Mn(dbm)_3$[h]							
exptl	1800	1710	430	−4.35	0.26	1.97	1.99
calcd method 1[c]				−3.80		1.96	1.99
calcd method 2[d]				−1.35		1.96	1.99
calcd method 3[e]				−4.59 (−4.84)			

[a] Ligand-field parameters D_q, D_s, and D_t are defined by Ballhausen.[37] [b] Ligand-field parameters determined by electronic absorption spectroscopy of Cr^{2+} sulfate, chloride, bromide, iodide, and perchlorate aqueous solutions;[18] zfs and g values determined here by HF-EPR of sulfate and chloride frozen solutions. McClure originally reported $D_q = 1400\ cm^{-1}$ for aqueous Cr^{2+}.[40] [c] Method 1: D and g_z values are calculated by exact solution of the Hamiltonian in eq 2; $g_{x,y}$ values are calculated by first-order perturbation theory derived from eq 2 as given by eq 3a. [d] Method 2: D and g values are calculated by perturbation theory as given by eq 3b, which does not include spin−spin coupling. [e] Method 3: D_{tot} value is given, which is the sum of D (method 2) and D' calculated by inclusion of $^3T_{1g}$ excited-state mixing as given by eq 4, with Racah parameters both from McClure[40] ($B = 810\ cm^{-1}$ (Cr^{2+}), $965\ cm^{-1}$ (Mn^{3+}); $C = 3565\ cm^{-1}$ (Cr^{2+}), $4450\ cm^{-1}$ (Mn^{3+})) and from Mabbs and Collison[41] ($B = 830\ cm^{-1}$ (Cr^{2+}), $1140\ cm^{-1}$ (Mn^{3+}); $C = 3400\ cm^{-1}$ (Cr^{2+}), $3650\ cm^{-1}$ (Mn^{3+})), the latter set giving values in parentheses, which are closer to those used by Barra et al.[14] [f] Ligand-field parameters determined by electronic absorption spectroscopy for the isostructural Cu^{2+} complex;[38] zfs and g values determined by single-crystal EPR for the Cr^{2+} complex. The negative sign for D is assumed.[23,24] [g] Ligand-field parameters determined by electronic absorption spectroscopy;[43] no EPR data are available. [h] Ligand-field parameters determined by electronic absorption spectroscopy; zfs and g values determined by polycrystalline HF-EPR.[14]

unsuccessful.) The effect of this tetragonal distortion on the electronic structure of both $[Cr(H_2O)_6]^{2+}$and $CrSO_4\cdot 5H_2O$ will be discussed below.

The crystal structure of $CrSO_4\cdot 5H_2O$ further shows a very slight rhombic distortion, as evidenced by the two sets of Cr−O_{aquo} bond lengths. This distortion may be related to the small rhombic zfs parameter ($|E| = 0.1\ cm^{-1}$) reported in the previous EPR study of this complex.[23] In contrast, we found no evidence for rhombic zfs in the present study of $[Cr(H_2O)_6]^{2+}$ (perpendicular EPR transitions are quite sensitive to this effect, and the simulations did not warrant $|E| > 0$). Therefore, $[Cr(H_2O)_6]^{2+}$ is likely a rigorously axial system, which makes it totally EPR-silent at conventional frequencies and fields, as opposed to integer-spin systems with significant E values, for which low-field $\Delta M_S > 1$ transitions can often be observed.[35,36]

We next turn to the electronic structure of $[Cr(H_2O)_6]^{2+}$ using a simple ligand-field model, as applied by Fackler and Holah in analyzing the electronic absorption spectra of this ion.[18] Chromium(II) is a ^5D state free ion that is split by an octahedral field into ^5E_g (t_2^3 e) and $^5T_{2g}$ (t_2^2 e^2) states. A tetragonal distortion further splits the ^5E_g state into $^5B_{1g}$ and $^5A_{1g}$ states and the $^5T_{2g}$ state into $^5B_{2g}$ and ^5E_g states in D_{4h} symmetry. The energies of these orbital states are given by Ballhausen[37] and are shown in Figure 5. This orbital ordering is appropriate for a tetragonal elongation, which is favored over a compression based on the crystallographic data for Cr^{2+} complexes.[22,32,33] The orbital energies in Figure 5 are those calculated for aqueous Cr^{2+} using the parameters determined by Fackler and Holah (Table 1).[18] The corresponding ligand-field values have not been reported for $CrSO_4\cdot 5H_2O$; however, Holmes and McClure determined them for the isomorphous crystal $CuSO_4\cdot 5H_2O$, which has a ^2E ground state similarly susceptible to Jahn−Teller distortion.[38] We therefore report these values in Table 1 and employ them below to calculate hypothetical zfs and g values for $CrSO_4\cdot 5H_2O$ for comparison with the experimental data,

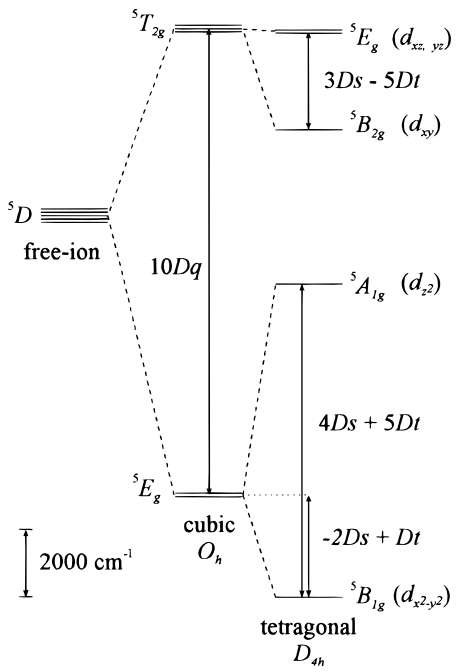

Figure 5. Energy levels of the Cr^{2+} ion as a free ion ($3d^4$, ^5D) and in cubic (O_h) and axial (tetragonal, D_{4h}) ligand fields. The ligand-field parameters are those of Ballhausen,[37] and the scaling is based on the values determined for aqueous Cr^{2+} by Fackler and Holah.[18] The d orbital labels correspond to the occupancy of the electron "hole" in high-spin $3d^4$.

(35) Münck, E.; Surerus, K.; Hendrich, M. P. *Methods Enzymol., C* **1993**, *227*, 463−474.
(36) Dexheimer, S. L.; Gohdes, J. W.; Chan, M. K.; Hagen, K. S.; Armstrong, W. H.; Klein, M. P. *J. Am. Chem. Soc.* **1989**, *111*, 8923−8925.
(37) Ballhausen, C. J. *Introduction to Ligand Field Theory*; Ballhausen, C. J., Ed.; McGraw-Hill: New York, 1962; pp 99−103.
(38) Holmes, O. G.; McClure, D. S. *J. Chem. Phys.* **1957**, *26*, 1686−1694.

realizing that these ligand-field parameters for Cu^{2+} do not necessarily correspond to those for the authentic Cr^{2+} complex.

The orbital states that result from ligand-field operators can be combined with the electron spin states to yield a complete description of the electronic system, from which zfs and g values can be determined. The Hamiltonian combining these ligand-field, spin−orbit, and electronic Zeeman interactions is given by[2]

$$H = B_4\{O_4^0 + 5O_4^4\} + B_2^0O_2^0 + B_4O_4^0 + \lambda(\mathbf{L}\cdot\mathbf{S}) - \rho\{(\mathbf{L}\cdot\mathbf{S})^2 + (1/2)(\mathbf{L}\cdot\mathbf{S}) - (1/3)(L(L+1)S(S+1))\} + \beta\mathbf{B}\cdot(\mathbf{L} + g_e\mathbf{S}) \quad (2)$$

where g_e is the free electron g value and O_k^q are the orbital operators appropriate for a tetragonally distorted cubic ligand field with splitting parameters $D_q = 12B_4$, $D_s = 3B_2^0$, $D_t = -12B_4^0$.[2,37] For Cr^{2+} and Mn^{3+} ($3d^4$, ^5D), $L = 2$, $S = 2$, the spin−orbit coupling constant $\lambda = 58$ cm^{-1} (Cr^{2+}) and 88 cm^{-1} (Mn^{3+}),[2] and the spin−spin coupling constant $\rho = 0.42$ cm^{-1} (Cr^{2+}) and 0.8 cm^{-1} (Mn^{3+}).[39] Inclusion of this spin−spin coupling term does not say much about its physical origin. In the framework of a spin Hamiltonian approach, spin−spin coupling is formally equivalent to the effects of mixing brought about by higher-order spin−orbit coupling terms.[2]

Second-order perturbation theory (first-order for the g values) applied to this Hamiltonian gives the following relations:[2]

$$D = -3(\rho + \lambda^2/\Delta)\cos 2\delta$$

$$E = -\sqrt{3(\rho + \lambda^2/\Delta)\sin 2\delta}$$

$$g_x = g_e - 2(\lambda/\Delta)(\cos\delta - \sqrt{3}\sin\delta)^2$$

$$g_y = g_e - 2(\lambda/\Delta)(\cos\delta + \sqrt{3}\sin\delta)^2$$

$$g_z = g_e - 8(\lambda/\Delta)\cos^2\delta \quad (3a)$$

where Δ is the energy gap between the cubic field $^5T_{2g}$ excited state (i.e., its tetragonal splitting is neglected) and the tetragonal field ground state and δ is a mixing parameter resulting from an orthorhombic distortion so that the ground state is described by $\{\cos\delta|^5B_{1g}\rangle + \sin\delta|^5A_{1g}\rangle\}$.[2] For Cr^{2+}, the observation that $E \approx 0$ means that δ is either 0 or 90°, which respectively correspond to a $^5B_{1g}$ ground state (the electron "hole" in the $3d_{x^2-y^2}$ orbital) or to a $^5A_{1g}$ ground state (the electron "hole" in the $3d_{z^2}$ orbital). The experimental determination here of the negative sign of D unequivocally indicates that $\delta = 0$ so that Cr^{2+} indeed has a $^5B_{1g}$ ground state, as expected for tetragonal elongation. On the basis of the structure of isomorphous $CuSO_4\cdot5H_2O$, $D < 0$ simply was assumed in the early study of $CrSO_4\cdot5H_2O$.[23] Use of eq 3a with $\delta \equiv 0$ (the experimental E gives $\delta \approx 0.74°$ for $CrSO_4\cdot5H_2O$), the free ion values for Cr^{2+}, and $\Delta \approx 14\,000$ cm^{-1} gives calculated values for $D = -1.98$ cm^{-1}, $g_y \equiv g_x = 1.99$ and $g_z = 1.97$, which are in reasonably good agreement with the experimental values.

To test this model for high-spin $3d^4$ systems more precisely, we have written a computer program to solve the Hamiltonian in eq 2 exactly by matrix diagonalization at various magnetic fields. We use the experimental D_q, D_s, and D_t values for $[Cr(H_2O)_6]^{2+}$ and those for $CuSO_4\cdot5H_2O$ as representative of $CrSO_4\cdot5H_2O$ (Table 1). Values for D are easily obtained from a zero-field calculation and confirmed by the intercept obtained using low parallel fields ($0 < B_\parallel \le 0.3$ T). This method (method 1) gives $D = -2.08$ and -2.04 cm^{-1} for $CrSO_4\cdot5H_2O$ and $[Cr(H_2O)_6]^{2+}$, respectively, which differ from the experimental values by ~7%. The g values are obtainable in principle from the slope of the energy levels as a function of field ($g_\parallel = \Delta E/(\beta\Delta B_\parallel)$), but these are difficult to determine in practice because the energies are so sensitive to spin−orbit coupling and field-induced state mixing, particularly with $B_\perp$. For example, low parallel fields ($0.1 \le B_\parallel \le 0.5$ T) give $g_z \approx 1.93$, while high fields ($10 \le B_\parallel \le 15$ T) give $g_z \approx 1.97$. Only high perpendicular fields ($10 \le B_\perp \le 15$ T) can be used meaningfully to calculate $g_{x,y}$, for which values of 1.93−1.98 are obtained. As mentioned above, it is correspondingly difficult to determine experimental g values. For example, the slope of the "$|-2\rangle \rightarrow |-1\rangle\perp$" transition (resonance H in Figures S1 and S2) gives an effective $g = 1.986$, while the slope of the "$|-2\rangle \rightarrow |-1\rangle\parallel$" transition (resonance B in Figures S1 and S2) gives $g = 1.945$. The simulation value $g = 1.98$ best accommodates the entire powder pattern spectrum at multiple frequencies and corresponds adequately to theoretically predicted values. There is thus good agreement overall between the electronic parameters determined by EPR and those calculated from Cr^{2+} ^5D free-ion parameters combined with 3d orbital energy levels determined by electronic absorption spectroscopy.[18] This indicates a consistent picture of the electronic structure of this ion, without the need for significant involvement of electronic excited states with lower spin multiplicity so that Cr^{2+} in these chemical environments approximates a pure high-spin $3d^4$ ion.

For comparison with the results of Barra et al.,[14] who used a somewhat different approach and obtained different conclusions for their system, we have used the above methods to calculate zfs and g values for $Mn(dbm)_3$ (with $\Delta \approx 18\,000$ cm^{-1} and $\delta \equiv 0$; the experimental E gives $\delta \approx 0.99°$ for $Mn(dbm)_3$), which are also given in Table 1. The D value calculated in this way, by including spin−spin coupling (method 1), differs from the experimental value by ~14%, twice as great a discrepancy as found above for Cr^{2+} (see Table 1). Barra et al.[14] did not specifically include spin−spin coupling in the form of eq 2. Their perturbation theory equations included more exact consideration of the 3d orbital energies, and their equations are given below, in slightly modified form to correspond more closely with eq 3a.

$$D = -(\lambda^2/2)\{8/\Delta E(xy) - 1/\Delta E(xz) - 1/\Delta E(yz)\} \approx -\lambda^2\{4/(10D_q) - 1/(10D_q + 3D_s - 5D_t)\}$$

$$E = (\lambda^2/2)\{1/\Delta E(xz) - 1/\Delta E(yz)\}$$

$$g_x = g_e - 2\{\lambda/\Delta E(yz)\} = g_e - 2\{\lambda/(10D_q + 3D_s - 5D_t + D_r)\}$$

$$g_y = g_e - 2\{\lambda/\Delta E(xz)\} = g_e - 2\{\lambda/(10D_q + 3D_s - 5D_t - D_r)\}$$

$$g_z = g_e - 8\{\lambda/\Delta E(xy)\} = g_e - 8\{\lambda/(10D_q)\} \quad (3b)$$

where $\Delta E(xy)$ corresponds to the energy difference between the given orbital and the $^5B_{1g}$ ground state and D_r is a rhombic splitting term. As found by Barra et al. for $Mn(dbm)_3$,[14] eq 3b gives unacceptable values for D in Cr^{2+}, off by nearly 70% (see Table 1, method 2). This disagreement between the above

(39) Pryce, M. H. L. *Phys. Rev.* **1950**, *80*, 1107−1108.

theoretical model and experiment was overcome by Barra et al. by directly including the effect of mixing in lower spin multiplicity electronic excited states (there are no excited quintet states). Many such states might potentially contribute, with excited triplet states being the most viable, in particular the triplet free-ion excited states (^{3}P, ^{3}F, ^{3}G, ^{3}H) that can give a $^3T_{1g}$ (LS $3d^4$) state in a cubic field. In a purely cubic field, the ^5E_g (t_2^3 e) ground state lies at an energy $E_E = (-6D_q - 21B)$, and when off-diagonal matrix elements are neglected, the $(^3H)^3T_{1g}$ (t_2^4) excited state lies at an energy $E_{T2} = (-16D_q - 15B + 5C)$, where B and C are the Racah parameters, taken either from McClure[40] or from Mabbs and Collison.[41] The ground and excited states are thus separated by $\Delta E(^3T_1) = (-10D_q + 6B + 5C) \approx 8000-9000$ cm^{-1} for Cr^{2+} and 7000−10000 cm^{-1} for Mn^{3+}, which is a sufficiently low energy to potentially be significant. As done by Barra et al.[14] and similarly by Dugad et al. in a magnetic susceptibility study of Mn(III) porphyrins,[42] the contribution of this excited state to the zfs, D', is given by[14]

$$D' = -\zeta^2/(6B + 5C + \Delta E(^5E_g - {}^5A_{1g})) = -\zeta^2/([10D_q - D_s - 10D_t] + 6B + 5C) \quad (4)$$

where the single-electron spin−orbit coupling constant is $\zeta =$ 236 cm^{-1} (Cr^{2+}) or 360 cm^{-1} (Mn^{3+}).[40] This gives $D' = -3.24$ cm^{-1} for Mn^{3+}, which with D from eq 3b yields $D_{tot} = D + D' = -4.6$, which is within ∼7% of the observed value, and an exact calculation gave even closer agreement.[14] In contrast, for Cr^{2+}, $D' \approx -2$ cm^{-1}, yielding $D_{tot} = -2.8$, which still differs by ∼20% from the observed value (see Table 1, method 3). Thus, the low-spin excited state of aqueous Cr^{2+} does not contribute to the ground state nearly as much as in $Mn(dbm)_3$. The Cr^{2+} system is rigorously axial ($|E/D| = 0$), while the Mn^{3+} complex has a significant rhombic zfs term ($|E/D| = 0.06$); this distortion may allow more extensive excited-state mixing.

Conclusions

High-field EPR spectroscopy has been used to probe the non-Kramers, $S = 2$, Cr^{2+} ion in frozen aqueous solution. The high-quality spectra obtained here show the applicability of HF-EPR to investigating aqueous solutions of integer-spin ("EPR-silent") transition metal complexes, such as could be obtained in metalloprotein samples. Previous HF-EPR studies have employed powder or single-crystal samples. Detailed analysis of the experimental spectra, based on a combination of analytical and full-matrix solutions to the spin Hamiltonian for an $S = 2$ system, gave zero-field splitting parameters $D = -2.20(5)$ cm^{-1}, $E = 0.0(1)$ cm^{-1}, and $g_\perp = g_\parallel = 1.98(2)$, independent of the counterion (chloride and sulfate) and the presence of glycerol. A pioneering single-crystal EPR study[23,24] of $CrSO_4 \cdot 5H_2O$ was unable to determine unequivocally the sign of D, but the magnitude was quite close to that seen here for $[Cr(H_2O)_6]^{2+}$; however, the solid showed a measurable E value, indicating an orthorhombic distortion that is absent in solution. The combination of the present HF-EPR data with a previous electronic absorption spectroscopic study[18] provides a complete picture of the electronic structure of Cr^{2+} in this chemical environment. These results show that aqueous Cr^{2+} has octahedral hexaaquo coordination, with tetragonal elongation, as expected by Jahn−Teller theory[37] and structural data for related Cr^{2+} complexes.[22,32,33] The results are also compared to a recent study of a Mn^{3+} complex, $Mn(dbm)_3$, which showed that electronic excited states affect the ground state of the complex.[14] This was found to be much less the case with Cr^{2+} complexes, which may be the result of their more rigorously axial symmetry.

Acknowledgment. This work was supported by The Human Frontier Science Program (RG-349/94 to L.-C.B.) and the NHMFL (L.A.P., J.K., and L.-C.B.). J.T. is supported by Roosevelt University and the NHMFL User Program. We thank Dr. H. Weihe of the H. C. Ørsted Institute, Copenhagen, Denmark for providing us with the EPR simulation program.

Supporting Information Available: Figure showing a complete spectral data set for aqueous Cr^{2+} sulfate (Figure S1), plot showing the resonant field/frequency points for that data set with linear fits (Figure S2), and figure showing HF-EPR spectra of microcrystalline $CrSO_4 \cdot 5H_2O$ (Figure S3) (4 pages). Ordering information is given on any current masthead page.

IC9806683

(40) McClure, D. S. *Solid State Phys.* **1959**, *9*, 399−525.
(41) Mabbs, F. E.; Collison, D. *Electron Paramagnetic Resonance of d Transition Metal Compounds*; Elsevier: Amsterdam, 1992.
(42) Dugad, L. B.; Behere, D. V.; Marathe, V. R.; Mitra, S. *Chem. Phys. Lett.* **1984**, *104*, 353−356.
(43) Fackler, J. P., Jr.; Chawla, I. D. *Inorg. Chem.* **1964**, *3*, 1130−1134.